# COMPARISON OF THREE ARCHITECTURES OF THERMALLY INTEGRATED PUMPED THERMAL ENERGY STORAGES USING SIMULATION

Frédéric Ransy*, Vincent Lemort
[1] University of Liege, Thermodynamics Laboratory, Liege, Belgium
* *Corresponding Author: frederic.ransy@uliege.be*

**Abstract.** This paper compares three architectures of Thermally Integrated Pumped Thermal Energy Storages (TI-PTES) by simulating their performance and changing the waste heat and storage temperatures. The key performance indicators include the power-to-power efficiency, the volumetric energy density, and the waste heat ratio. The systems based on low-temperature storages are suitable for industrial processes with a high waste heat ratio, while the high temperature storage system provides higher energy density and is suitable for low waste heat ratio.

**Keywords.** Thermally Integrated Carnot Battery, simulation, waste heat, industrial process

**Nomenclature**

*Abbreviations*

| | |
|---|---|
| CAES | Compressed Air Energy Storage |
| COP | Coefficient of Performance |
| HP | Heat Pump |
| LCOS | Levelized cost of storage |
| ORC | Organic Rankine Cycle |
| PCM | Phase Change Material |
| PHES | Pumped Hydro Energy Storage |
| PtP | Power-to-Power Efficiency |
| TI- | Thermally Integrated |
| PTES | Pumped Thermal Energy Storage |
| TRL | Technology Readiness Level |
| VEB | Volumetric Energy Density |

*Symbols*

| | |
|---|---|
| t | Duration (h) |
| T | Temperature (°C) |
| V | Volume (m³) |
| $\dot{W}_{el}$ | Electric power (W) |

*Subscripts*

| | |
|---|---|
| ch | charge |
| dis | discharge |
| tot | total |

## 1 Introduction

A pumped thermal energy storage is an energy storage system that stores electrical energy in form of heat. To do so, the system utilizes a HP to convert electricity into thermal energy, which is stored in one or two tanks. Then, the thermal energy is converted back to electricity through a heat-to-power cycle. As explained by Dumont et al. [1], this technology is suitable for medium and long storage duration (from 4 to 8 h or more). It has no environmental constraints (no need of an existing reservoir or cave), but the efficiency and the TRL compared to CAES and PHES are lower. Different configurations have been proposed in the literature, and many commercial projects are currently developed. Indeed, Novotny et al. [2] reviewed in 2022 more than 30 on-going projects from the kW to the MW scale with several TRL. In these systems, the PtP lies between 30 and 60 %. To increase the efficiency, a solution consists of integrating in the process a waste heat, for instance from an industrial process. Korhan et al. [3], Shuozhuo et al. [4] and Frate et al. [5] showed PtP higher than 80 %. The increase in efficiency is due to a higher COP of the HP in charging mode thanks to the utilization of the waste heat. The efficiency of this energy storage, called Thermally Integrated Pumped Thermal Energy Storage, is highly dependent on the process in which it is integrated, but also on parameters such as the waste heat temperature or the thermodynamic cycle architecture.

## 2 Methodology

This paper compares three different TI-PTES architectures and shows the impact of several parameters on the system performance, evaluated through three performance indicators.

### 2.1 *Proposed TI-PTES architectures*

Figure 1 shows the three TI-PTES architectures simulated in this paper. Those architectures are well described in the literature, and are suitable for waste heat integration.

The first system (top in Figure 1) considers a vapor compression HP for charging, two pressurized liquid water storage tanks and an ORC with preheater for discharging. The working fluid for both the cycles is R1233zd(E). As explained by Liang et al. in [6], this fluid is a good compromise between efficiency, low equipment size and pressure ratio.

The second system (middle in Figure 1) considers the same fluid and thermodynamic architecture as in the first system (vapor compression HP + ORC), but with an additional latent storage with PCM.

The third system (bottom in Figure 1) considers a reversed Brayton cycle HP with supercritical $CO_2$ as working fluid for charging, two sensible molten salt storage tanks and a steam Rankine cycle for discharging. This system presented in [7] has a potential theoretical PtP of at least 50 %.

### 2.2 *Simulation model description*

The simulation models consist of determining at each point in the systems the thermodynamic state (pressure, enthalpy, entropy, etc.). Each component is modeled in steady state in considering the energy and the mass balances. For the heat exchangers, the temperature profiles are computed and a minimum pinch point, considered constant, is imposed. Pressure drops are not considered. The pumps, compressors and turbines are modeled with a constant isentropic efficiency. The heat losses are not computed. Expansion valves are considered as isenthalpic. The heat losses in the storage tanks are considered through a constant efficiency. In the cycle, constant ORC subcooling and superheating HP/ORC are imposed. The HP subcooling is optimized to maximize the efficiency.

### 2.3 *Performance indicators definitions*

Three performance indicators are generally utilized to define the performance of TI-PTES: the PtP, the VED and the LCOS. The latter is not considered in this paper. In the case of TI-PTES, the waste heat ratio is another indicator to consider. All these indicators are defined based on the energy exchanged over 1 charge/discharge cycle, which depends on the charging and discharging durations. These parameters depend on the application of the TI-PTES. In this paper, photovoltaic integration service is supposed, with a charging duration $t_{ch}$ of 7 h and a discharging duration $t_{dis}$ of 8 h.

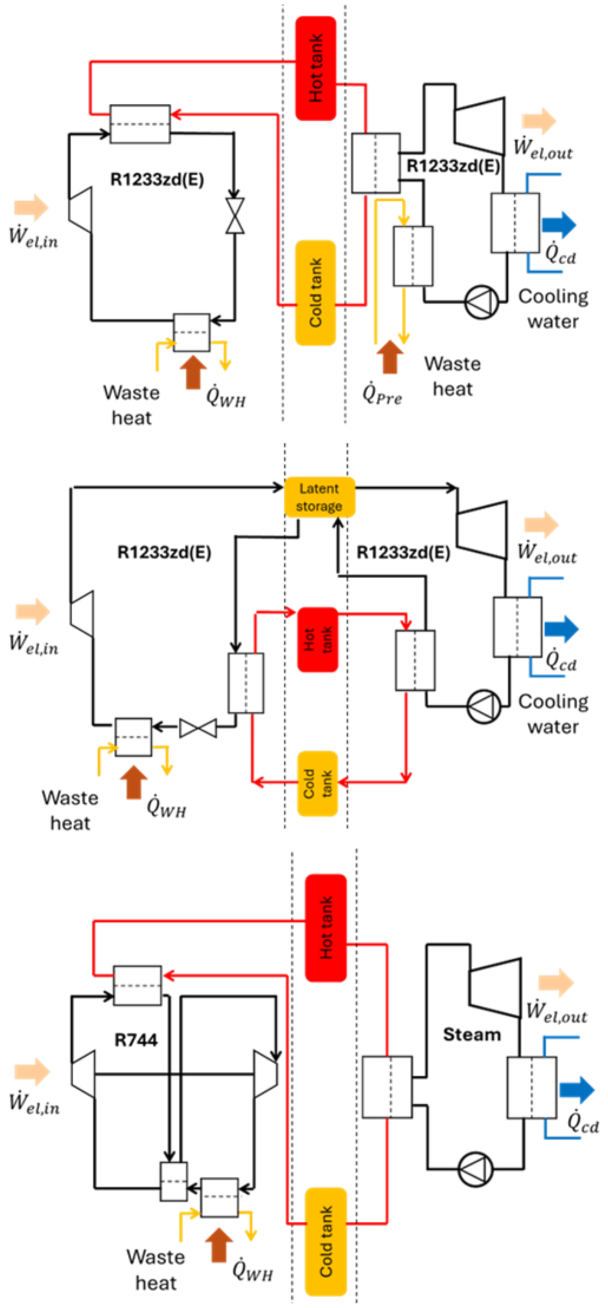


**Figure 1**: The three TI-PTES architectures. Top: system 1. Middle: system 2. Bottom: system 3

Based on the energy powers defined in Figure 1, the three performance indicators are defined as:

$$PtP = \frac{\dot{W}_{el,out}\, t_{dis}}{\dot{W}_{el,in}\, t_{ch}} \tag{1}$$

$$VED = \frac{\dot{W}_{el,out}\, t_{dis}}{V_{tank,tot}} \tag{2}$$

$$f_{waste} = \frac{\dot{Q}_{WH}\, t_{ch} + \dot{Q}_{Pre}\, t_{dis}}{\dot{W}_{el,out}\, t_{dis}} \tag{3}$$

The PtP expresses the power-to-power efficiency, and is computed with the net inlet and outlet electrical energies. The VED expresses the electrical energy released by the system in relation with the total system volume, taking into account the sensible and latent storage tanks $V_{tank,tot}$. The waste heat ratio expresses the ratio between the amount of waste heat energy necessary during charging and the amount of electric energy released during discharging. This factor indicates how a Carnot Battery architecture can effectively be integrated in a given industrial process, characterized by an electric energy need and a waste energy potential.

### *2.4 Parameters and boundary conditions*

The parameters defining the system components and the boundary conditions for the three architectures are summarized in Table 1. The inlet waste heat temperature, which has a considerable impact on the results, is varied between 50°C and 90°C. The storage temperature is also varied. The maximum and minimum storage temperatures are constrained by technological limitations and the storage materials. For the systems 1 and 2, as water is considered as the storage material, the storage temperature is limited from minimum 70 °C to maximum 140 °C. For the system 1, the min/max storage temperature difference between the two tanks is 25/50°C, respectively. As explained in [8], in this range, the LCOS of the system is minimized. For system 3, as molten salt is considered as the storage material, the storage temperature is limited from minimum 300°C to maximum 540°C. The storage temperature difference between the two tanks is varied between 140 K and 240 K.

**Table 1:** Parameters imposed in the models

| Item | Symbol | Value |
|---|---|---|
| Compressor efficiency | $\eta_{is,comp}$ | 80 % |
| Motor efficiency | $\eta_{motor}$ | 98 % |
| Turbine efficiency | $\eta_{is,turb}$ | 85 % |
| Generator efficiency | $\eta_{gen}$ | 98 % |
| Pump efficiency | $\eta_{is,pump}$ | 70 % |
| Heat storage efficiency | $\eta_{sto}$ | 95 % |
| Pinch points in HX's (systems 1 and 2, **or** 3) | $\Delta T_{pp}$ | 3 or 20 K |
| Superheating degree HP/ORC | $\Delta T_{SH}$ | 8 K |
| Subcooling degree ORC | $\Delta T_{SC}$ | 2 K |
| Discharging power capacity | $\dot{W}_{el,out}$ | 1 MW |
| Input cooling water temperature | $T_{w,cw,su}$ | 20°C |
| Cooling water temperature lift | $\Delta T_{cw}$ | 10 K |
| Inlet waste heat temperature | $T_{w,WH,su}$ | 50-90°C |
| Waste heat temperature lift | $\Delta T_{WH}$ | 10 K |

## 3 Results and discussion

This section presents the three performance indicators described in section 2.3 for the three architectures. In all figures, system 1 is in orange, system 2 in blue and system 3 in green. The results are similar to the work conducted in [8] and [9].

Figure 2 represents the variation of the PtP (top) and the waste heat ratio (bottom) with the inlet waste heat temperature. In Figure 2, for the systems 1, 2 and 3, the storage temperatures are fixed to 90-140°C (1), 103°C (2), and 305-540°C (3), respectively. For systems 1 and 2, the PtP curves are similar, and the inlet waste heat temperature has a strong impact. Indeed, the PtP is multiplied by 214 % when the waste heat temperature changes from 50 to 90°C. However, for system 3, the PtP is only multiplied by 108 %. Concerning the waste heat ratio $f_{waste}$, for each system, it increases with the waste heat temperature. Moreover, this indicator is highly dependent on the system considered and lies between 0.5 and 8.

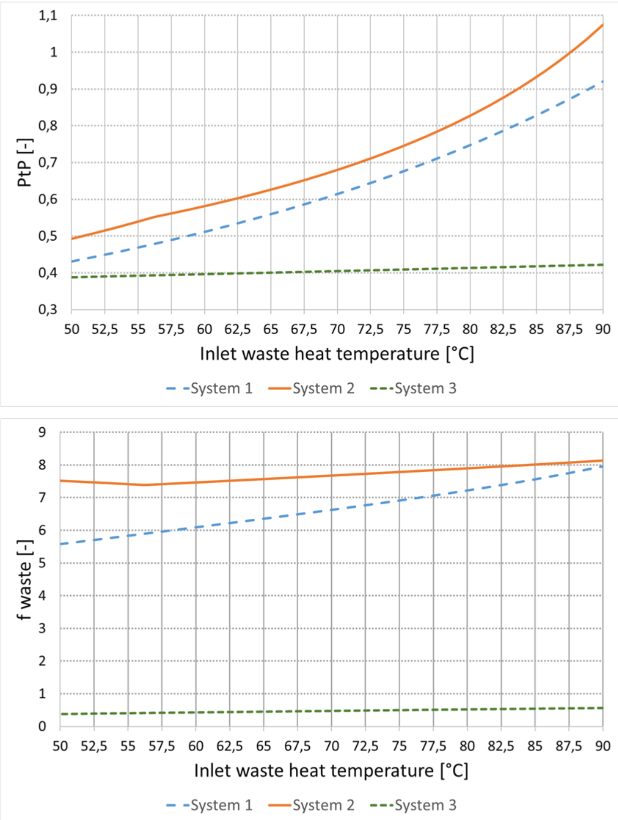


**Figure 2:** Variation of PtP (top) and waste heat ratio (bottom) with the inlet waste heat temperature

Figure 3 represents the operating envelopes for the three systems. These maps represent the PtP and the VED as a function of the waste heat ratio $f_{waste}$. The orange, blue and green surfaces represent, for the three architectures, all the possible performance indicator values when the storage and the waste heat temperatures are varied within the ranges described in the section 2.4. The system 1 and 2 are characterized by high values of PtP and waste heat ratio, and also large variations of these factors. However, the VED is lower with small variations. For the system 3, it is the opposite. Indeed, the PtP and the waste heat ratio are small with small variations, while the VED is much higher with large variations. These maps can be utilized to successfully chose and design the architecture of a TI-PTES according to the characteristics of the industrial process.

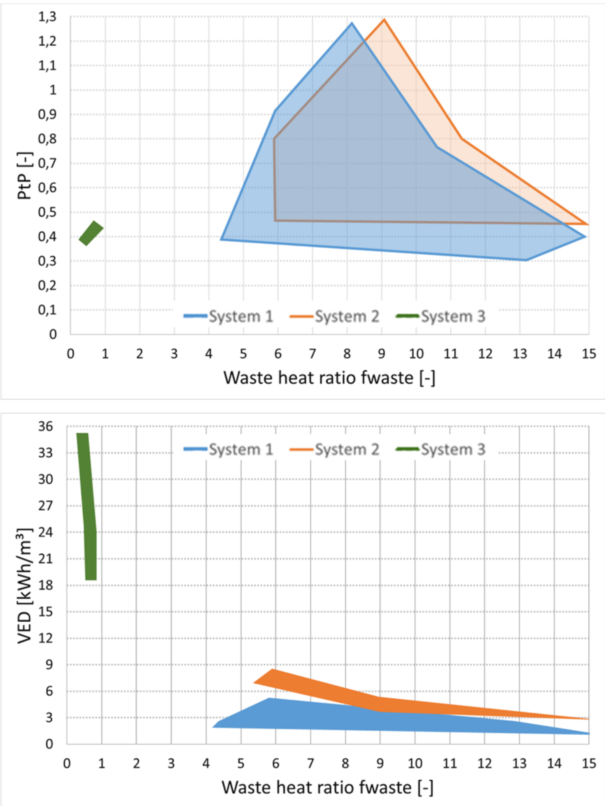


**Figure 3:** Operating envelope for the three systems. Top: PtP. Bottom: VED

## 4 Conclusion

This paper compares three TI-PTES architectures to help in the choice and design of such system when integrated in an industrial process. The systems 1 and 2 should be chosen for industrial processes with waste heat ratio higher than 4. In that case, the choice between 1 and 2 depends on the desired VED. The efficiency of such system will be highly dependent on the waste heat temperature, and this impact must not be omitted during the design phase. For industrial processes with waste heat ratio lower than 1, the system 1 is the most appropriate. In that case, the waste heat temperature has a much lower impact on the efficiency. To complete the analysis, a future work will consist of calculating the LCOS for the three architectures, and also adding technical constraints on the thermodynamic cycles, such max/min operating pressures and temperatures.

## References


[1] Dumont O. et al., "Carnot battery technology: A state-of-the-art review.", in Journal of Energy Storage, Vol. 32, 2020.

[2] Novotny V. et al., "Review of Carnot Battery Technology Commercial Development", in Energies, 2022.

[3] Korhan Ökten and Burak Kurşun, "Thermo-economic assessment of a thermally integrated pumped thermal energy storage system combined with an absorption refrigeration cycle driven by low-grade heat source", in Journal of Energy Storage, Vol 51, 2022.

[4] Shuozhuo Hu et al., "Thermo-economic analysis of the pumped thermal energy storage with thermal integration in different application scenarios", in Energy Conversion and Management, Vol. 236, 2021.

[5] Frate, G.F. et al., " Rankine Carnot Batteries with the Integration of Thermal Energy Sources: A Review", in Energies , 13, 2020.

[6] Ting Liang et al., "Key components for Carnot Battery: Technology review, technical barriers and selection criteria", in Renewable and Sustainable Energy Reviews, Volume 163, 2022.

[7] Aga V. et al., "Supercritical CO2-Based Heat Pump Cycle for Electrical Energy Storage for Utility Scale Dispatchable Renewable Energy Power Plants", in 5th International Symposium - Supercritical CO2 Power Cycles, San Antonio, Texas, 2016.

[8] Yuemao Jiang et al., "Enhanced thermally integrated Carnot battery using low-GWP working fluid pair: Multi-aspect analysis and multi-scale optimization", in Applied Energy, Volume 376, Part A, 2024.

[9] Shuozhuo Hu et al., "Thermo-economic analysis of the pumped thermal energy storage with thermal integration in different application scenarios", in Energy Conversion and Management, Volume 236, 2021.